The interaction between lithium acceptors and gallium donors in zinc oxide

T. N. Sky, K. M. Johansen (iD), Y. K. Frodason, B. G. Svensson, and L. Vines

View Online   Export Citation   CrossMark

ARTICLES YOU MAY BE INTERESTED IN

The interaction between lithium acceptors and gallium donors in zinc oxide

T. N. Sky,[a)] K. M. Johansen, Y. K. Frodason, B. G. Svensson, and L. Vines
Department of Physics/Center for Materials Science and Nanotechnology, University of Oslo, P.O. Box 1048 Blindern, N-0316 Oslo, Norway

Diffusion of lithium (Li) in uniformly gallium (Ga)-doped monocrystalline bulk zinc oxide (ZnO) is studied over a wide temperature range (500–1150 °C) and is demonstrated to be dictated by the distribution of Ga. Below 800 °C, the indiffusion of Li from a Li-doped ZnO sputtered film into n^+ single crystalline ZnO yields an abrupt and compensated Li-doped box region with the Li concentration matching the free-electron concentration, in accordance with several previous experimental and theoretical reports. However, experimental observations of Li-diffusion at higher temperatures reveal a dissociative diffusion mechanism for heat treatments up to 1150 °C. By employing a reaction-diffusion model that includes both Li and Ga, a dissociation energy of 4.6 eV is obtained from the experimental Li diffusion data. This is in excellent agreement with theoretical results for the dissociation of $(\mathrm{Li_{Zn}Ga_{Zn}})^0$ (4.8 eV) into Li_i^+ and $(\mathrm{Ga_{Zn}V_{Zn}})^-$ and suggests that this neutral and stable acceptor-donor pair prevails in Li- and Ga-doped ZnO. *Published by AIP Publishing.*
https://doi.org/10.1063/1.5063326

I. INTRODUCTION

The behavior of lithium (Li) in crystalline zinc oxide (ZnO) has been studied for many decades, with the first report on experimental Li diffusion as early as 1960.[1] Both donor and acceptor properties of Li were observed early on and it was suggested that Li substituting Zn ($\mathrm{Li_{Zn}}^-$) and interstitial Li (Li_i^+) was the identity of the acceptor and donor states, respectively.[1] This amphoteric behavior of Li is now well established based on more recent experimental[2–4] and theoretical[5,6] results. Li has been shown to primarily reside on the Zn site in n-type ZnO,[4] demonstrating the self-compensating effect of Li, with $\mathrm{Li_{Zn}}^-$ being favorable when the Fermi level (ϵ_F) is close to the conduction band minimum (CBM) and under oxygen rich conditions, while Li_i^+ would prevail for ϵ_F close to the valence band maximum (VBM) and under Zn-rich conditions.

Li diffusion in ZnO has previously been studied at temperatures up to 600 °C by Lander[1] and Knutsen *et al.*[7] under Zn-rich and O-rich conditions, respectively. In both reports, the diffusion of Li was described by assuming Li_i^+ to be the mobile species, while $\mathrm{Li_{Zn}}^-$ was considered immobile in the studied temperature range. The model assumed a kick-out mechanism between substitutional Zn by mobile Li_i^+ into stable $\mathrm{Li_{Zn}}^-$ and highly mobile Zn_i^{2+} (the migration barrier of 0.55 eV[8]), with extracted Li_i^+ migration barriers of 0.98 eV[1] and 1.34 eV[7] reported for the two studies, respectively.

Theoretical results by Carvalho *et al.*[6] using hybrid functional calculations reported an ionization energy of 0.6–1.1 eV for $\mathrm{Li_{Zn}}^-$, while a migration barrier of 0.6–0.7 eV for the diffusion of Li_i^+ was found. In addition, they further suggested that under O-rich conditions, the dominant diffusion process corresponds to a dissociative mechanism requiring a substantial activation energy. However, such a diffusion

mechanism would be observed at higher temperatures than that previously reported.

In this work, we have used secondary ion mass spectrometry (SIMS) and hybrid density functional theory (DFT) to study the diffusion of Li into the single crystal Ga-doped bulk ZnO containing very low residual Li concentration in the as-grown state. The background concentration of Ga donors made it possible to investigate the diffusion of Li at Fermi-level positions close to CBM, i.e., wherein the interstitial configuration is expected to be highly unfavorable. Unlike previously reported experiments on Li diffusion in ZnO, the present study addresses the diffusion mechanisms of Li diffusion in the temperature range of 850–1150 °C, evidencing a dissociative mechanism that has not previously been shown experimentally. The results demonstrate that the diffusion of Li is controlled by the concentration and distribution of Ga, resulting in a close to one-to-one ratio between the Li and Ga concentrations at moderate temperatures. Combining the experimental SIMS results with hybrid DFT results using a reaction-diffusion type model,[9,10] the diffusion of Li is evidenced to proceed by a dissociative donor-vacancy assisted diffusion mechanism, where mobile Li_i^+ reacts with more stable $(\mathrm{Ga_{Zn}V_{Zn}})^-$ pairs to produce neutral $(\mathrm{Li_{Zn}Ga_{Zn}})^0$ pairs. A dissociation energy barrier of 4.6 eV is extracted in the modelling of the experimental data, which is in excellent agreement with the theoretical predictions of 4.8 eV for the dissociation of $(\mathrm{Li_{Zn}Ga_{Zn}})^0$.

II. METHODS

A. Experimental

A thin film of Li-doped ZnO ($\sim 2 \times 10^{20}\,\mathrm{cm}^{-3}$) was deposited onto a hydrothermally grown single crystalline ($000\bar{1}$-oriented) bulk ZnO wafer, containing an as-grown uniform Ga concentration of $1 \times 10^{19}\,\mathrm{cm}^{-3}$ with a measured charge carrier concentration of $8 \times 10^{18}\,\mathrm{cm}^{-3}$. The as-grown

a)t.n.sky@fys.uio.no

bulk wafers were obtained from the authors of Ref. 11, produced/grown using a modified hydrothermal method, resulting in a low residual Li concentration ($< 1 \times 10^{15}$ cm^{-3}). The deposition of the Li-rich thin film was carried out in a Semicore magnetron sputtering system using a Li-doped ZnO target ($Zn_{0.95}Li_{0.05}O$) with a purity of 99.95%, resulting in a $0.3\,\mu$m thick Li-doped ZnO film. After the deposition, the wafer was cleaved into two smaller samples (labelled A and B) by the use of a Rofin PowerLine E-25 SHG laser cutter. Sample A was sequentially heat treated for 15 min from 500 °C up to 800 °C in stages of 50 °C, while sample B received a similar procedure but at higher temperatures (850–1150 °C) and for longer times (30 min). A Cameca IMS7f Secondary Ion Mass Spectrometer (SIMS) equipped with a O$_2$ primary ion beam source was used to record the concentration vs depth profiles of Li and Ga. Absolute concentration values were obtained by measuring Li and Ga implanted reference samples, ensuring less than $\pm 10\%$ error in accuracy. For depth calibration, the sputtered crater depths were determined by a Dektak 8 stylus profilometer and a constant erosion rate was assumed.

B. Theoretical

First-principles calculations were performed by using the Heyd-Scuseria-Ernzerhof (HSE)[12] hybrid functional and the projector augmented wave method,[13–15] as implemented in the VASP code.[16,17] The fraction of the screened Hartree-Fock exchange was set to $\alpha = 37.5\%$,[18] which yields a bandgap (3.42 eV) and lattice parameters ($a = 3.244$ Å and $c = 5.194$ Å) that are in excellent agreement with experimental values.[19,20] All defect calculations were performed using a plane-wave energy cutoff of 500 eV, a special k-point at $k = (\frac{1}{4}, \frac{1}{4}, \frac{1}{4})$, and a 96-atom-sized wurtzite supercell.[21] Defect formation energies were calculated by following the well established formalism outlined in Refs. 22 and 23. For instance, the formation energy of Li$_{Zn}$ in charge-state q is given by

$$E_f(\text{Li}_{Zn}^q) = E_{tot}(\text{Li}_{Zn}^q) - E_{tot}^{bulk} + \mu_{Zn} - \mu_{Li} + q\epsilon_F, \quad (1)$$

where $E_{tot}(\text{Li}_{Zn}^q)$ and E_{tot}^{bulk} denote the total energy of the defect-containing and pristine supercells, and μ_{Zn} and μ_{Li} are the chemical potential of the removed Zn- and added Li-atom, respectively. For charged defects, we applied the anisotropic[24] Freysoldt-Neugebauer-Van de Walle finite-size correction.[25,26] Oxygen rich conditions are considered, where μ_{Zn} corresponds to the total energy per the bulk metallic Zn atom plus the formation enthalpy of ZnO, i.e., $\mu_{Zn} = E_{tot}(Zn) + \Delta H_f(ZnO)$. The solubility of Li is limited by the formation of Li$_2$O, and under oxygen rich conditions $\mu_{Li} = E_{tot}(Li) + \frac{1}{2}\Delta H_f(\text{Li}_2O)$. Similarly, the solubility of Ga is limited by the formation of Ga$_2$O$_3$ and thus $\mu_{Ga} = E_{tot}(Ga) + \frac{1}{2}\Delta H_f(\text{Ga}_2O_3)$.

III. RESULTS AND DISCUSSION

A. Li diffusion at moderate temperatures

Figure 1 shows the Li and Ga concentration vs depth profiles for the sample isocronally heat treated (15 min) at
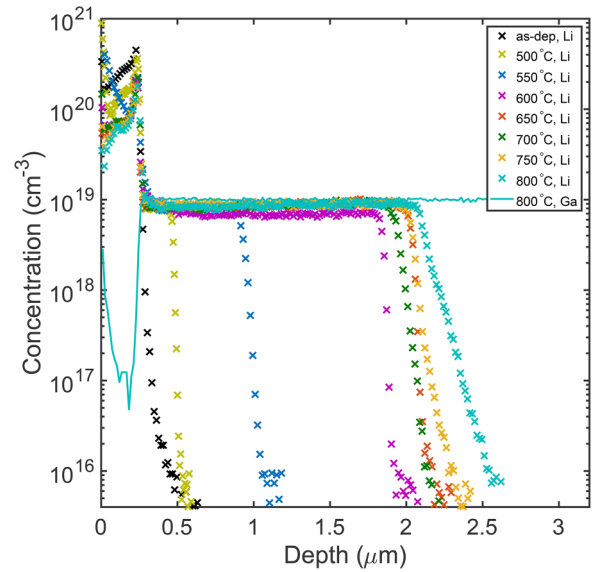

FIG. 1. Experimental Li and Ga concentration vs depth profiles of sample A isochronally heat treated (15 min) at temperatures 500–800 °C.

temperatures in the range 500–800 °C, as measured by SIMS. Already at 500 °C, Li starts to migrate from the 0.3 μm thick Li-doped ZnO film into the Ga-doped ZnO bulk. At these temperatures, Ga is practically immobile (cf. Ref. 10) showing only a slight out-diffusion to the film at 800 °C. The concentration of Li in the plateau of the very distinct box-like Li diffusion profiles is about 8–9×10^{18} cm^{-3} for all temperatures. Treatments up to 600 °C show a gradual increase in the effective diffusion length. However, at temperatures between 650 °C and 800 °C, only a small increase in the effective diffusion length is observed, indicating a depletion of mobile Li in the film. Furthermore, above 700 °C, a tail start to develop in the deep end of the Li box-profiles, indicative of a different process emerging at higher temperatures. This unfortunately limits the possibility to extract reliable diffusion parameters. However, the general diffusion behavior of Li at moderate temperatures (Fig. 1) is in accordance with that observed in previous reports,[1,7] where the diffusion of Li was explained to proceed by fast diffusing Li$_i^+$, while Li$_{Zn}^-$ is practically immobile below 600 °C. In particular, it was found in Ref. 7 that the characteristic level at which the concentration of Li changes abruptly was correlated with the background concentration of ionized donors. Indeed, the experimental results presented in Fig. 1 strongly support this notion and further demonstrate that in the presence of a background doping of Ga, the diffusion of Li follows the concentration and distribution of Ga.

Experimental and theoretical studies of the amphoteric behavior of Li reported in the literature[2–6] show that high doping levels of Li lead to a highly compensated material. Indeed, the Li-doped ZnO film is shown to be highly resistive by 4-point probe measurements, with Li as the primary impurity. This suggests the presence of both Li$_{Zn}^-$ and Li$_i^+$ in the film. Mobile Li$_i^+$ will diffuse into the n-type bulk; however, Li$_i^+$ will be highly unfavorable and is expected to convert into a more energetically favorable configuration, e.g., the substitutional Zn-site,

ensuring continued indiffusion from the film. Moreover, Fig. 1 suggests that Li is trapped by a defect stable up to $\sim 750\,°C$ after entering the bulk crystal, in good agreement with previous experiments.[1,7]

B. Li diffusion above 800 °C

Figure 2(a) shows the Li and Ga concentrations vs depth profiles for sample B after isochronal heat treatments (30 min) in the temperature range 850–1150 °C. After the 850 °C treatment, Li shows similar distinct box-like diffusion behavior as that observed for sample A above (Fig. 1). Note that the total amount of indiffused Li in sample B at 850 °C is higher ($\sim 1\,\mu m$ deeper profile) than that observed for sample A at the same temperature (Fig. 1). The reason for this difference may be attributed to an outdiffusion of Li from the deposited film due to a longer accumulated diffusion time in sample A compared to B. Nevertheless, this difference will not affect our analysis below. Increasing the temperature above 950 °C clearly reveals that Li starts to redistribute, and the profiles extend over $20\,\mu m$ into the bulk after the 1150 °C treatment. As shown in Fig. 2(b), the integrated concentration of Li within the indiffused profiles is effectively maintained at all temperatures, demonstrating that no additional influx of Li occurs from the film (or the outflux from the bulk) after the initial 850 °C treatment. This ensures a clear boundary condition, making it highly suitable to apply diffusion modelling.

Interestingly, the evolution of the Ga distribution within the initial indiffused box-region [Fig. 2(a)] shows a correlation to that of the Li distribution, or rather vice versa. The redistribution of Ga is observed for treatments exceeding 850 °C, in accordance with previous results[10] reporting a migration barrier of 2.4 eV for $(Ga_{Zn}V_{Zn})^-$ in ZnO. In addition to the out diffusion of Ga causing a gradient in the Ga distribution toward the film, Ga also forms a distinct pattern at the interface between the Li doped and undoped bulk material. This is particularly prominent after the 950 °C and 1000 °C treatments [see the redistribution at $3-4\,\mu m$ shown in Fig. 2(c)], before it disappears again at higher temperatures. These features may be indicative of the presence of a considerable potential gradient across the Li-rich and Li-lean regions, as previously suggested for Li-doped ZnO.[7]

1. Theoretical predictions of prevalent defects

To get an overview of likely defect configurations that may be responsible for the initial Li "trapping" and subsequent apparent dissociation at higher temperatures, theoretical calculations using comparable conditions (oxygen-rich) were conducted. Figure 3(a) shows the formation energy vs the Fermi-level position (ϵ_F) for relevant defects, as obtained from hybrid DFT calculations. As can be seen, Li_i^+ is highly unfavorable under n-type conditions (ϵ_F close to CBM) and will readily convert into any of the more energetically favorable configurations Li_{Zn}^- or $(Li_{Zn}Ga_{Zn})^0$, if encountering either V_{Zn}^{2-} or $(Ga_{Zn}V_{Zn})^-$, respectively. The calculated stability of these substitutional Li-related defects is shown in Fig. 3(b), where the removal energy E_r and dissociation energy E_d of Li_{Zn}^- and $(Li_{Zn}Ga_{Zn})^0$ are given as a function of
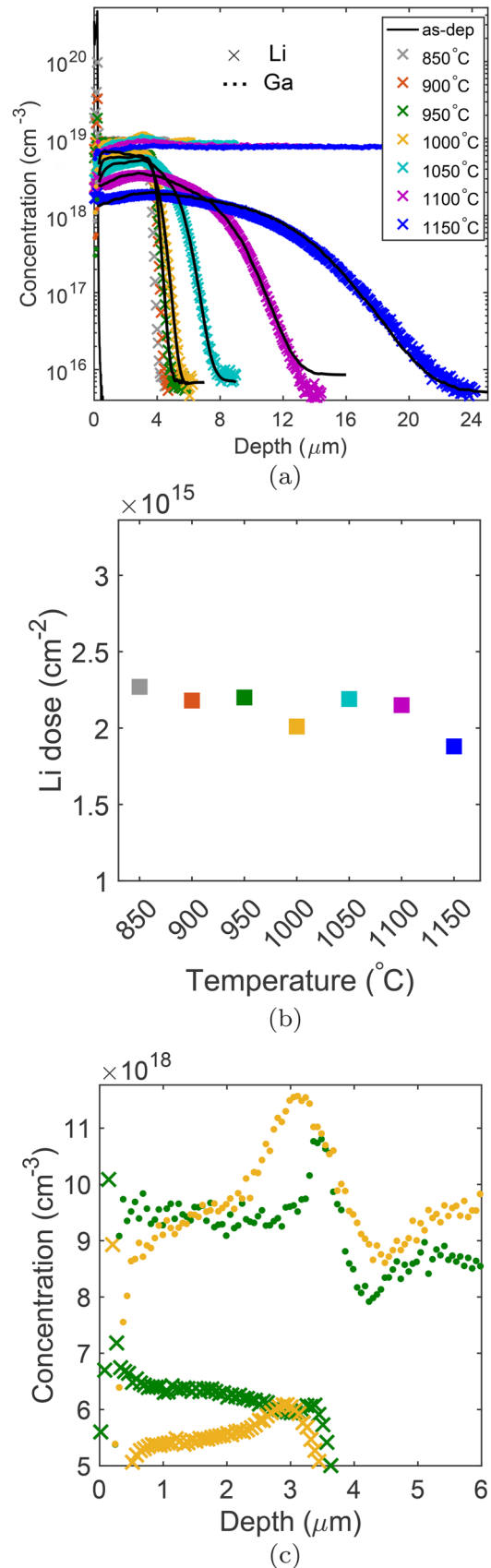

FIG. 2. (a) Experimental Li and Ga concentration vs depth profiles of sample B isochronally heat treated (30 min) at temperatures 850–1150 °C. The solid lines show the best fit of the reaction-diffusion model [Eq. (2)]. The integrated Li concentration within the Li depth profiles is shown in (b), and (c) shows a zoomed view of the junction region for the 950 and 1000 °C profiles (others excluded for clarity).
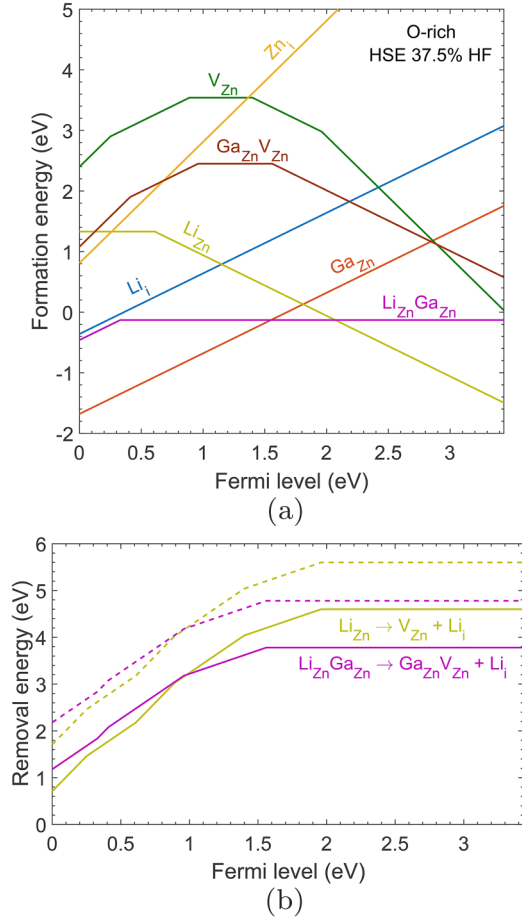
FIG. 3. (a) Predicted formation energies as a function of Fermi-level position for typical defects present in Li- and Ga-doped ZnO. (b) The resulting energy required to remove Li from the Zn-site to the interstitial site, with or without Ga_{Zn}^+ as a next nearest neighbor, as represented by the solid lines. The dotted lines show the overall dissociation energy, which include the migration barrier of ~ 1 eV for the diffusion of Li_i^+.

ϵ_F. Here, E_r is defined as the energy required to convert the substitutional Li to an interstitial position, but not completely dissociate, which also necessitates the inclusion of the smallest migration barrier for the involved constituents, i.e., the migration of either Li_i, V_{Zn}, or $Ga_{Zn}V_{Zn}$. From Fig. 3(b), $E_r(Li_{Zn}^-) = 4.6$ eV and $E_r[(Li_{Zn}Ga_{Zn})^0] = 3.8$ eV in the n-type ZnO, with the respective E_d being ~ 1 eV higher when considering the previously reported migration barrier of Li_i^+ (see Ref. 1), provided that Li_i^+ leave behind the V_{Zn}-related defect. It is interesting to note that, at highly compensated conditions (ϵ_F pinned close to mid-bandgap), $(Li_{Zn}Ga_{Zn})^0$ is the most energetically favorable configuration. However, the dominating trap for Li_i^+ strongly depends on the availability of the isolated vacancy vs the donor-vacancy pair.

2. Reaction diffusion model

Motivated by the above indications of V_{Zn}^{2-} or $(Ga_{Zn}V_{Zn})^-$ being involved in the diffusion of Li, the experimental diffusion data in Fig. 2(a) have been analyzed using a reaction-diffusion model[9,10,27] assuming a dissociative diffusion mechanism. The diffusion of Li assisted by V_{Zn}-related defects (X) can be described by reaction-diffusion equations

(see, e.g., Refs. 9, 10, and 27–31 for a similar and general treatment)

$$\frac{\partial C_X}{\partial t} = KC_{V_{Zn}}C_{Li_i} - vC_X,$$

$$\frac{\partial C_{Li_i}}{\partial t} = D_{Li_i}\frac{\partial^2 C_{Li_i}}{\partial x^2} - \frac{\partial C_X}{\partial t}, \quad (2)$$

where $v = v_0 e^{-E_d(X)/k_BT}$ is the dissociation rate for X [i.e., either Li_{Zn}^- or $(Ga_{Zn}Li_{Zn})^0$], with v_0 being the attempt frequency (on the order of $\sim 10^{13}$ s^{-1}) and $E_d(X)$ the activation energy for dissociation of X. In Eq. (2), the reaction constant $K = 4\pi R_c D_{Li_i}$ is the formation rate of X, where R_c is the coulomb force assisted effective reaction radius set to 1 nm, and $D_{Li_i} = 2 \times 10^{-2}\exp(-0.98\,\text{eV}/k_BT)\,\text{cm}^2\,\text{s}^{-1}$ is the diffusivity of interstitial Li, as obtained by Lander,[1] and is used as a fixed parameter in the simulations. In Eq. (2), it is assumed that the formation of V_{Zn}^{2-} is the limiting process for the formation of $(Ga_{Zn}V_{Zn})^-$, i.e., $(Ga_{Zn}V_{Zn})^-$ forms instantaneously after the formation of V_{Zn}^{2-} at the studied temperatures, due to the high concentration of Ga_{Zn}^+. Thus, the diffusion model is not sensitive to whether Li is captured by V_{Zn}^{2-} or $(Ga_{Zn}V_{Zn})^-$. In the simulations, C_X is determined from the preceding Li-profile with the integrated concentration of the Li being constant, as seen in Fig. 2(b). That is, the flux of Li_i at the interface is set to zero (except for the 1150 °C, where a slight outdiffusion has been considered).

In order to solve the above RD equations [Eq. (2)], a value for $C_{V_{Zn}}(x, t)$ is required. Profiles of $C_{V_{Zn}}(x, t)$ can be estimated from DFT estimates of the V_{Zn}^{2-} formation energy in Fig. 3(a). That is, the distribution of V_{Zn}^{2-} can be expressed as[9,27]

$$C_{V_{Zn}}(x, t) = N_s e^{-[E_f(V_{Zn}^{2-})/k_BT]}\left(\frac{n(x, t)}{N_c(T)}\right)^2, \quad (3)$$

where N_s is the number of substitutional zinc lattice sites, $n = C_{Li_i} - 2C_{V_{Zn}} + C_{Ga_{Zn}}$ accounts for the net charge carrier concentration of the system with $C_{Ga_{Zn}} \approx C_{Ga} - C_X$, and N_c is the effective density of states in the conduction band. This implies that an instantaneous equilibrium of $C_{V_{Zn}}$ is established and governed by ϵ_F. The vacancy formation energy can then be expressed as $E_f(V_{Zn}^{2-}) = E_{f,0}(V_{Zn}^{2-}) - 2\epsilon_F$, where $E_{f,0}(V_{Zn}^{2-})$ is the formation energy at the valence band edge, set to 6.9 eV in our simulations as obtained from Fig. 3(a) and also guided by previous DFT reports.[21,32–34] For a more detailed discussion of the reaction-diffusion model used in this work, see Refs. 9, 10, and 27

The considerations above leave only the dissociation rate v as the unknown fitting variable to solve Eq. (2). Figure 4 shows the extracted v vs the inverse absolute temperature, obtained from the best fits of the experimental data in Fig. 2(a). This results in a dissociation energy of 4.6 ± 0.2 eV with a prefactor of $v_0 = 5 \times 10^{15}$ s^{-1} for the diffusion of Li. Using the relation for Gibb's free energy $G = H - TS$, with an enthalpy H and entropy S, the dissociation rate can be expressed as $v = v_0 e^{-G/k_BT} = \Gamma_0 e^{S/k_B}e^{-H/k_BT}$, where $\Gamma_0 \approx 10^{13}$ s^{-1} is the characteristic frequency of the lattice. Thus, the high value obtained for v_0 may suggest a contribution from the entropy (S) for the dissociation process. In this
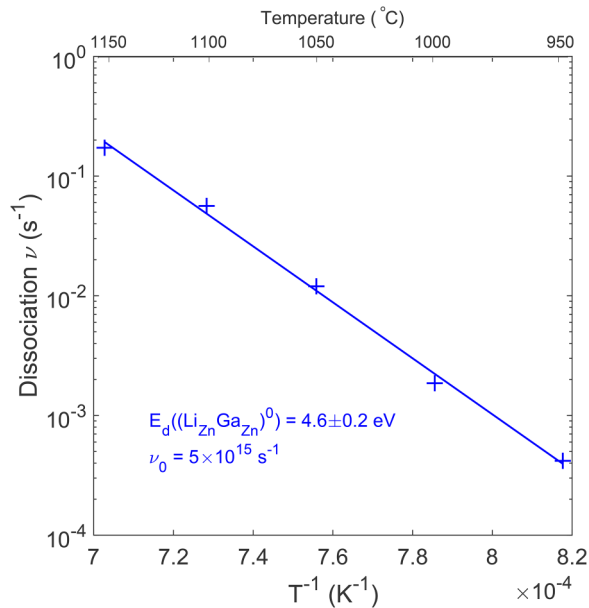
FIG. 4. Dissociation frequencies $\nu_{\mathrm{Li_{Zn}Ga_{Zn}}}$, as a function of the inverse absolute temperature.

regard, previous experimental studies of Ga-doped ZnO[27,35] show that Ga-doping strongly enhances the Zn self-diffusion in ZnO and, in particular, that the diffusion prefactor scales with the Ga-concentration. These results, supported by the present study, indicate that the presence of Ga in the ZnO lattice affects the vibrational entropy, thus enhancing the diffusivity of both intrinsic- and impurity related defects. It can also be mentioned that theoretical studies of silicon carbide have previously shown that the entropy contribution for self-diffusion is significant at high temperatures ($\sim 0.6T_m$, where T_m is the melting temperature),[36] suggesting that such effects may also be important for other material systems at comparable conditions.

By comparing the extracted value of 4.6 ± 0.2 eV (Fig. 4) with the DFT results in Fig. 3(b), this excludes the possibility that $\mathrm{Li_{Zn}}^-$ is the dissociating defect, as this would imply a migration barrier for either Li_i or $\mathrm{V_{Zn}}$ that is close to zero (i.e., the dissociation energy is the sum of the removal and migration barriers). On the other hand, this result is in excellent agreement with the sum of the migration barrier of Li_i^+ of ~ 1 eV and the energy barrier of 3.8 eV as found from the DFT results in Fig. 3(b) for the removal of Li from $(\mathrm{Li_{Zn}Ga_{Zn}})^0$. Hence, we conclude that $(\mathrm{Li_{Zn}Ga_{Zn}})^0$ is the dominating Li-related defect in Li- and Ga-doped ZnO.

IV. CONCLUSION

Diffusion of Li in the single crystal Ga-doped ZnO is experimentally demonstrated to depend on the concentration and distribution of Ga. Indiffusion of Li at temperatures from 500 °C up to 800 °C from a Li-doped ZnO deposited film into n^+ ZnO yields an abrupt and compensated Li-doped box region with a Li concentration matching the as-grown free-electron concentration. The diffusion of Li is well described by employing a reaction-diffusion model that accounts for the

presence of both Li and Ga. Using previous experimental results[1] for the Li_i^+ migration barrier, we obtain an activation energy of 4.6 ± 0.2 eV with a prefactor of $\nu_0 = 5 \times 10^{15}$ s^{-1} for the dissociation process mediating for the Li diffusion. This is in excellent agreement with our DFT results predicting an energy of 4.8 eV for the dissociation of $(\mathrm{Li_{Zn}Ga_{Zn}})^0$ into Li_i^+ and $(\mathrm{Ga_{Zn}V_{Zn}})^-$, thus evidencing $(\mathrm{Li_{Zn}Ga_{Zn}})^0$ to be the assisting defect for the dissociative diffusion of Li.

[1]J. J. Lander, J. Phys. Chem. Solids **15**, 324 (1960).
[2]P. T. Neuvonen, L. Vines, A. Y. Kuznetsov, B. G. Svensson, X. Du, F. Tuomisto, and A. Hallén, Appl. Phys. Lett. **95**, 242111 (2009).
[3]L. Vines, E. V. Monakhov, R. Schifano, W. Mtangi, F. D. Auret, and B. G. Svensson, J. Appl. Phys. **107**, 103707 (2010).
[4]K. M. Johansen, A. Zubiaga, I. Makkonen, F. Tuomisto, P. T. Neuvonen, K. E. Knutsen, E. V. Monakhov, A. Y. Kuznetsov, and B. G. Svensson, Phys. Rev. B **83**, 245208 (2011).
[5]M. G. Wardle, J. P. Goss, and P. R. Briddon, Phys. Rev. B **71**, 155205 (2005).
[6]A. Carvalho, A. Alkauskas, A. Pasquarello, A. K. Tagantsev, and N. Setter, Phys. Rev. B **80**, 195205 (2009).
[7]K. E. Knutsen, K. M. Johansen, P. T. Neuvonen, B. G. Svensson, and A. Y. Kuznetsov, J. Appl. Phys. **113**, 023702 (2013).
[8]D. G. Thomas, J. Phys. Chem. Solids **3**, 229 (1957).
[9]K. M. Johansen, L. Vines, T. S. Bjorheim, R. Schifano, and B. G. Svensson, Phys. Rev. Appl. **3**, 024003 (2015).
[10]T. N. Sky, K. M. Johansen, H. N. Riise, B. G. Svensson, and L. Vines, J. Appl. Phys. **123**, 055701 (2018).
[11]W. Lin, K. Ding, Z. Lin, J. Zhang, J. Huang, and F. Huang, CrystEngComm **13**, 3338 (2011).
[12]A. V. Krukau, O. A. Vydrov, A. F. Izmaylov, and G. E. Scuseria, J. Chem. Phys. **125**, 224106 (2006).
[13]P. E. Blöchl, Phys. Rev. B **50**, 17953 (1994).
[14]G. Kresse and J. Hafner, J. Phys. Condens. Matter **6**, 8245 (1994).
[15]G. Kresse and D. Joubert, Phys. Rev. B **59**, 1758 (1999).
[16]G. Kresse and J. Hafner, Phys. Rev. B **47**, 558 (1993).
[17]G. Kresse and J. Furthmüller, Phys. Rev. B **54**, 11169 (1996).
[18]F. Oba, A. Togo, I. Tanaka, J. Paier, and G. Kresse, Phys. Rev. B **77**, 245202 (2008).
[19]D. C. Reynolds, D. C. Look, B. Jogai, C. W. Litton, G. Cantwell, and W. C. Harsch, Phys. Rev. B **60**, 2340 (1999).
[20]J. Albertsson, S. C. Abrahams, and Å. Kvick, Acta Cryst. B **45**, 34 (1989).
[21]Y. K. Frodason, K. M. Johansen, T. S. Bjørheim, B. G. Svensson, and A. Alkauskas, Phys. Rev. B **95**, 094105 (2017).
[22]S. B. Zhang and J. E. Northrup, Phys. Rev. Lett. **67**, 2339 (1991).
[23]C. Freysoldt, B. Grabowski, T. Hickel, J. Neugebauer, G. Kresse, A. Janotti, and C. G. Van de Walle, Rev. Mod. Phys. **86**, 253 (2014).
[24]Y. Kumagai and F. Oba, Phys. Rev. B **89**, 195205 (2014).
[25]C. Freysoldt, J. Neugebauer, and C. G. Van de Walle, Phys. Rev. Lett. **102**, 016402 (2009).
[26]H.-P. Komsa, T. T. Rantala, and A. Pasquarello, Phys. Rev. B **86**, 045112 (2012).
[27]T. N. Sky, K. M. Johansen, B. G. Svensson, and L. Vines, "Influence of Fermi level position on vacancy-assisted diffusion of aluminum in zinc oxide," Phys. Rev. B (to be published).
[28]E. Antoncik, Appl. Phys. A **56**, 291 (1993).
[29]H. Bracht, Phys. Rev. B **75**, 035210 (2007).
[30]M. Uematsu, J. Appl. Phys. **82**, 2228 (1997).
[31]U. M. Gosele, Ann. Rev. Mater. Sci. **18**, 257 (1988).

[32]A. Janotti and C. G. Van de Walle, Phys. Rev. B **76**, 165202 (2007).

[33]D. O. Demchenko, B. Earles, H. Y. Liu, V. Avrutin, N. Izyumskaya, Ü. Özgür, and H. Morkoç, Phys. Rev. B **84**, 075201 (2011).

[34]D. Steiauf, J. L. Lyons, A. Janotti, and C. G. Van de Walle, APL Mater. **2**, 096101 (2014).

[35]A. Azarov, V. Venkatachalapathy, Z. Mei, L. Liu, X. Du, A. Galeckas, E. Monakhov, B. G. Svensson, and A. Kuznetsov, Phys. Rev. B **94**, 195208 (2016).

[36]E. Rauls, T. Frauenheim, A. Gali, and P. Deák, Phys. Rev. B **68**, 155208 (2003).